Myocardial O utilization and energetics of the left ventricle in hypertrophic cardiomyopathy

Güclü, A.

2017

Chapter 3

Gene-specific increase in the energetic cost of contraction in hypertrophic cardiomyopathy caused by thick filament mutations

A. Güçlü*
E.R. Witjas-Paalberends*
T. Germans
P. Knaapen
H.J. Harms
A.M.C. Vermeer
I. Christiaans
A.A.M. Wilde
C. dos Remedios
A.A. Lammertsma
A.C. van Rossum
G.J.M. Stienen
M. van Slegtenhorst
A.F.L. Schinkel
M. Michels
C.Y. Ho
C. Poggesi
J. van der Velden

*These authors contributed equally

Cardiovasc Res. 2014; 103:248-257

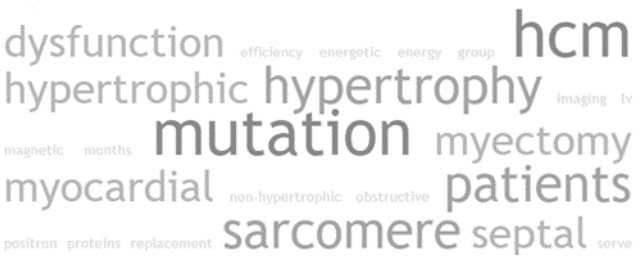

Abstract

Aims

Disease mechanisms regarding hypertrophic cardiomyopathy (HCM) are largely unknown and disease onset varies. Sarcomere mutations might induce energy depletion for which until now there is no direct evidence at sarcomere level in human HCM. This study investigated if mutations in genes encoding myosin binding protein C (*MYBPC3*) and myosin heavy chain (*MYH7*) underlie changes in the energetic cost of contraction in the development of human HCM disease.

Methods and results

Energetic cost of contraction was studied *in vitro* by measurements of force development and ATPase activity in cardiac muscle strips from 26 manifest HCM patients (11 $MYBPC3_{mut}$, 9 $MYH7_{mut}$, and 6 sarcomere mutation-negative, HCM_{smn}). In addition, *in vivo*, the ratio between external work (EW) and myocardial oxygen consumption (MVO_2) to obtain myocardial external efficiency (MEE) was determined in 28 pre-hypertrophic mutation carriers (14 $MYBPC3_{mut}$ and 14 $MYH7_{mut}$) and 14 healthy controls using [^{11}C]-acetate positron emission tomography and cardiovascular magnetic resonance imaging. Tension cost, i.e. ATPase activity during force development, was higher in $MYBPC3_{mut}$ and $MYH7_{mut}$ compared with HCM_{smn} at saturating [Ca^{2+}]. Tension cost was also significantly higher in $MYH7_{mut}$ at submaximal, more physiological [Ca^{2+}]. EW was significantly lower in both mutation carrier groups, while MVO_2 did not differ. MEE was significantly lower in both mutation carrier groups compared with controls, showing the lowest efficiency in *MYH7* mutation carriers.

Conclusion

We provide direct evidence that sarcomere mutations perturb the energetic cost of cardiac contraction. Gene-specific severity of cardiac abnormalities may underlie differences in disease onset and suggests that early initiation of metabolic treatment may be beneficial, in particular, in *MYH7* mutation carriers.

Introduction

Hypertrophic cardiomyopathy (HCM) is a genetically inherited cardiac disease with an incidence of 0.2%, characterized by asymmetric hypertrophy of the left ventricle in the absence of other cardiac or systemic diseases.[1] Since its first description in 1957 as a non-coronary heart muscle disease of unknown aetiology,[2] the major breakthrough with respect to its cause was the discovery of the first mutation in the gene (*MYH7*) encoding the sarcomeric protein β-myosin heavy chain (cMyHC) in 1990.[3] In subsequent years, many HCM-causing mutations have been found, mostly in genes encoding sarcomeric proteins.[4] Despite the discovery of multiple genetic defects, insights into the pathophysiological mechanisms that lead from sarcomere mutation to HCM phenotype are limited. This is partly due to the clinical heterogeneity of HCM, ranging from asymptomatic individuals to sudden cardiac arrest or development of overt cardiomyopathy at young age. Moreover, several clinical studies observed differences in disease onset between patients with mutations in the most frequently affected thick filament genes, *MYH7* and *MYBPC3* (encoding cardiac myosin-binding protein C: cMyBP-C), indicative for gene-specific differences in the clinical course of HCM.[5–9] A better understanding of the sarcomeric deficits, which initiate the development of HCM, may explain phenotypic differences and improve treatment at an early stage.

A complex chain of events may lead from defective sarcomeres to contractile dysfunction and cardiac remodelling. An attractive hypothesis that has been put forward is the energy depletion hypothesis, which originally was shown to be of importance in the development of heart failure.[10–13] The association of energy depletion with HCM mutations[14,15] is based on observations in both *in vivo* transgenic mouse models[16–19] and *in vivo* human studies.[20–22] Using magnetic resonance spectroscopy, a reduction in the cardiac PCr to ATP ratio, a measure of energetic status, was found both in mice with a mutation in the gene encoding the cardiac thin filament protein troponin T (*TNNT2*)[16,17] and in those harbouring the *MYH7* R403Q mutation,[18] compared with controls. Similarly, PCr/ATP was found to be reduced in HCM patients with left ventricular hypertrophy (LVH).[20–23]

Interestingly, a reduction in PCr/ATP was already present in mutation carriers without LVH.[20] Moreover, a recent study in *MYBPC3* mutation carriers without LVH showed reduced myocardial efficiency compared with controls, evident from a reduced ratio between cardiac work and oxygen consumption.[23] These studies suggest that changes in myocardial efficiency may represent a primary trigger of cardiac dysfunction and remodelling in HCM. To date, however, there is no direct proof of inefficient ATPase activity at the level of the cardiac sarcomere in human HCM.

To investigate whether sarcomere mutations increase an energetic cost of contraction, *in vitro* ATPase activity was measured during isometric sarcomere contraction in demembranated multicellular muscle strips from manifest sarcomere mutation-positive HCM patients. Sarcomere mutation-negative HCM patients served as a control group as they have the same phenotype as mutation-positive HCM patients, evident from similar left LV remodelling in the absence of a sarcomeric gene mutation. Moreover, to assess if gene-specific variation may underlie a difference in disease onset, comparisons were made between *MYBPC3* and *MYH7* mutations in the *in vitro* and *in vivo* study, using [^{11}C]-acetate positron emission tomography (PET) and cardiovascular magnetic resonance (CMR) imaging studies, in pre-hypertrophic mutation carriers compared with the healthy control subject.

Methods

In vitro analysis

Cardiac tissue of manifest HCM patients

Cardiac tissue was obtained from the LV interventricular septum of 26 HCM patients during myectomy surgery relieving LV outflow tract obstruction or after heart transplantation (three patients). Eleven patients harboured a mutation in *MYBPC3*, nine in *MYH7,* and six did not carry a sarcomeric gene mutation after screening eight most commonly involved genes. The latter, sarcomere mutation-negative patient group (HCM_{smn}) served as control. Specific mutation and clinical data of patients are provided in Table *1*. The study protocol was in agreement with principles outlined in the Declaration of Helsinki, and it was approved by the local Medical Ethics Review Committees. Written informed consent was obtained from each patient prior to surgery.

Simultaneous measurements of force production and ATPase activity

The solutions and equipment used for the functional measurements have been described previously.[24,25] Membrane-permeabilized cardiac muscle strips were stretched in the apparatus based on the passive force reaching 10% of the maximal calcium-activated force, which corresponds to a sarcomere length of ~2.2 µm.[26] Isometric force and ATPase activity were measured at saturating (pCa 4.5) and sub-saturating [Ca^{2+}] at 20°C. Example registrations of both force development and ATPase activity of a muscle strip are shown in Figure *1*. The muscle strip was activated in a saturating Ca^{2+} solution (pCa 4.5; 31.6 µmol·L^{-1}) until it reached a steady state and subsequently relaxed in a low [Ca^{2+}] solution (pCa 9; 1 nmol·L^{-1}) (Figure *1A*). Force was determined at the steady-state level and was normalized to

the cross-sectional area (CSA) of the muscle strip to calculate tension. The CSA of the preparation was estimated based on an elliptical shape, i.e. CSA = (width x depth x π)/4. Average dimensions (mean ± SD) of all muscle strips (n=118) were 1.4 ± 0.4 mm in length, 352 ± 60 μm in width and 309 ± 55 μm in depth.

ATPase activity was measured using an enzyme-coupled assay, in which ATP regeneration from ADP and phosphoenol-pyruvate by the enzyme pyruvate kinase is coupled with the oxidation of NADH to NAD and the reduction of pyruvate to lactate by L-lactic dehydrogenase, and was normalized to volume (length x CSA).[27] NADH oxidation (Figure *1B*) was measured photometrically from the absorbance at 340 nm of near-UV light. When the muscle strip was transferred into the activation solution, force developed and the NADH absorbance signal started to decline simultaneously. After returning the muscle strip into the relaxation solution, 0.5 nmol ADP was injected into the measuring bath to calibrate the absorbance signal. The Ca^{2+}-activated ATPase activity was calculated using the slope of the dotted regression line fitted to the absorbance signal when it reached a steady state. The basal ATPase activity was subtracted from the maximal ATPase activity at each [Ca^{2+}]. Basal ATPase activity was measured in relaxing solution (pCa 9.0). The economy of muscle contraction is expressed as tension cost (TC), i.e. the amount of ATP used during the development of force (normalized to CSA).

In vivo analysis

Pre-hypertrophic mutation carriers

This study population comprised 28 asymptomatic pre-hypertrophic mutation carriers. Mutation carriers were first-degree relatives of symptomatic HCM patients and were recruited after genetic testing. Fourteen carriers had a mutation in *MYBPC3* and 14 in *MYH7*. The LV wall thickness in all subjects was <10 mm. None of the carriers had systemic or other cardiac disease or used medication. In addition, 14 genotype-negative relatives of the mutation carriers were included as a control group. The study was approved by the Medical Ethics Review Committee of the VU University Medical Center, and all participants gave written informed consent prior to inclusion.

Table 1. Characteristics of manifest HCM patients

	Mutation	Type	Age	Sex	LVOT	ST
***MYBPC3*$_{mut}$**						
1	c.1458-1G>C	Truncation	41	F	92	22
2	c.927-2A>G	Truncation	48	M	82	18
3	c.2827C>T	Truncation	24	F	81	24
4	c.2373dupG	Truncation	32	M	88	23
5	c.2373dupG	Truncation	60	M	77	23
6	c.3407_3409del	Truncation	55	M	108	22
7	c.2864_2865delCT	Truncation	36	F	Na	Na
8	c.772G>A	Truncation	46	M	62	25
9	c.1020C>G	Truncation	51	F	110	29
10	c1999_2000delinsG	Truncation	61	F	85	23
11	c.2309_2A>G	Truncation	67	F	72	25
Mean ± SD			47 ± 13	6F/11	86 ± 15	23 ± 3
***MYH7*$_{mut}$**						
1	c.4130C>T	Missense	58	F	100	20
2	c.1816G>A	Missense	46	F	79	17
3	c.2360G>A	Missense	61	M	Na	Na
4	c.1208G>A	Missense	24	M	85	34
5	c.1208G>A	Missense	35	M	Na	Na
6	c.1208G>A	Missense	58	F	Na	Na
7	c.2345G>A	Missense	30	F	128	29
8	c.2080C>T	Missense	28	M	32	48
9	c.2080C>T	Missense	81	F	70	19
Mean ± SD			47 ± 19	5F/9	82 ± 32	28 ± 12
HCM$_{smn}$						
1			52	M	169	22
2			72	F	88	24
3			65	F	85	19
4			49	M	61	20
5			46	M	81	19
6			59	M	85	18
Mean ± SD			57 ± 10	2F/6	95 ± 38	20 ± 2

Age at time of surgery, F, female; M, male, LVOT, left ventricular outflow tract gradient in mmHg; ST, septal thickness in mm; Cardiac tissue collected during heart transplantation surgery, na, data not available.

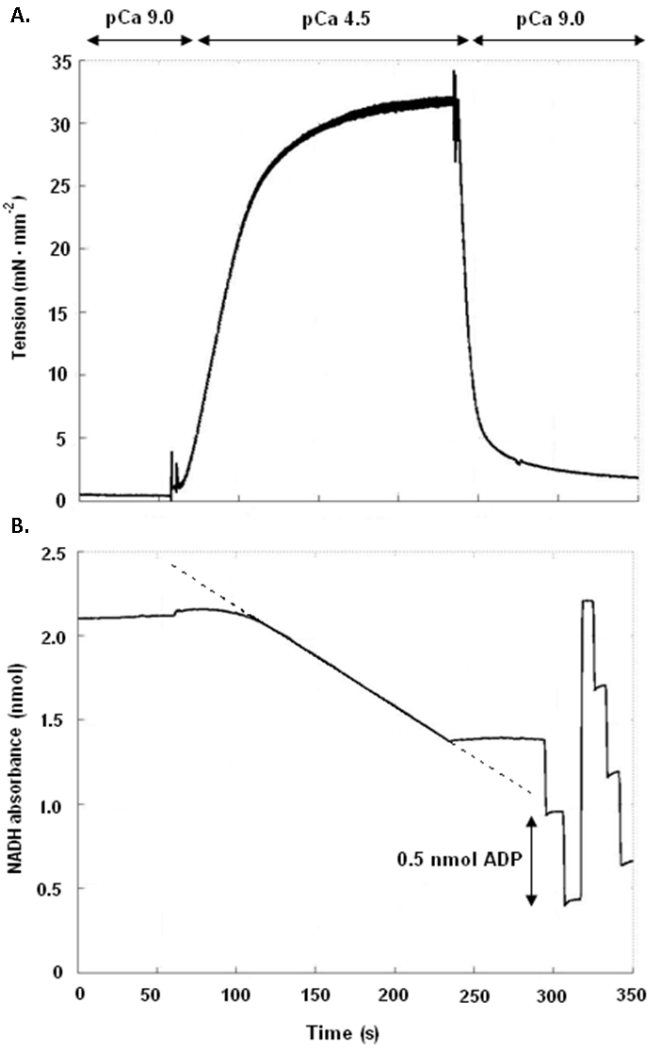

Figure 1. Functional recordings of a muscle strip. A. Force generation (normalized to CSA). **B.** NADH absorbance.

CMR and PET

The study protocol comprised [^{11}C]-acetate PET and CMR imaging.

CMR image acquisition

CMR was performed on a 1.5-Tesla whole body scanner (Magnetom Sonata or Avanto, Siemens, Erlangen, Germany), using a six-channel phased-array body coil.
After survey scans, a retro-triggered, balanced steady-state free precession gradient-echo sequence was used for cine imaging. Image parameters were: slice thickness 5 mm, slice gap 5 mm, temporal resolution <50 ms, repetition time 3.2 ms, echo time 1.54 ms, flip angle 60° and a typical image resolution of 1.3 by 1.6 mm. The cardiac cycle consisted of 20 phases. After obtaining 4-, 3-, and 2-chamber view cines, a contiguous short-axis steady-state free precession stack was acquired extending from the mitral valve annulus to the LV apex, to obtain LV mass (LVM) and enable volumetric analysis of the LV.[28] Cine images were acquired during breath-hold at mild expiration. Late gadolinium enhancement (LGE) images were acquired 10-15 minutes after intravenous administration of 0.2 mmol·kg^{-1} Gadolinium, using a two-dimensional segmented inversion-recovery prepared gradient-echo sequence. Inversion- recovery time was 250-300 ms.

CMR image analysis

Images were analysed off-line using the software package MASS (MR Analyical Software System; Medis, Leiden, The Netherlands). LV volume analysis was performed by manually drawing epicardial and endocardial contours on all end-diastolic (ED) and end-systolic (ES) LV short-axis images. Next, global LV function parameters, including ED volume (LVEDV), ES volume (LVESV), stroke volume (SV), LV ejection fraction (LVEF) and LV mass (LVM) were computed from the cine images. Each myocardial segment was evaluated for the presence of hyperenhancement, i.e. LGE, which is a measure of replacement fibrosis, defined as an area of signal enhancement greater than 5 SD of the signal of non-enhanced myocardium. The extent of LGE was expressed as the percentage of the total myocardial tissue area studied. Cardiac mechanical external work (EW) was calculated as the product of stroke volume and mean arterial pressure.

PET/CT image acquisition

For *MYH7* mutation carriers, [^{11}C]-acetate scans were obtained on a Gemini TF-64 PET/CT scanner (Philips Healthcare, Best, The Netherlands). Data of *MYBPC3*$_{mut}$ carriers and the control group were acquired as described previously.[23] All [^{11}C]-acetate PET scans were obtained after overnight fasting of patients. A 50 min list-mode emission scan was started simultaneously with a bolus injection of 370 MBq of

[^{11}C]-acetate (infusion speed 0.8 mL·s^{-1}) followed by a 35 mL saline flush (infusion speed 2 mL·s^{-1}). To correct for attenuation and scatter, the emission scan was followed immediately by a slow, respiration-averaged low dose CT scan (LD-CT, 55 mAs, rotation time 1.5 s, pitch 0.825, collimation 64x0.625, acquiring 20 cm in 12 s) during normal breathing. Data were reconstructed into 36 successive time frames (1x10, 8x5, 4x10, 3x20, 5x30, 5x60, 4x150, 6x300 s). Blood pressure and heart rate were recorded at regular intervals throughout the imaging procedures. Before PET acquisition, venous blood was withdrawn and NH_2-terminal pro-brain natriuretic peptide (NT-proBNP,), hemoglobin (Hb), creatinine, glucose, free fatty acid (FFA) and lactate levels were determined.

PET/CT image analysis

Input functions were obtained using in-house developed software. One cm diameter regions of-interest (ROIs) were placed over the ascending aorta in at least 5 transaxial image planes of the frame showing the first pass of the injected bolus. These ROIs were combined into one volume of interest (VOI) for the ascending aorta. A second set of ROIs was placed over the right ventricular (RV) cavity in 5 transaxial planes, with ROI boundaries at least 1 cm from the RV wall to avoid spill-over of myocardial activity. These ROIs were similarly combined into one RV VOI. Both VOIs were then transferred to the full dynamic images to obtain arterial whole blood ($C_A(t)$) and RV ($C_{RV}(t)$) time-activity curves. A correction for the fraction of non-metabolized [^{11}C]-acetate was applied to $C_A(t)$, based on data published by Sun and coworkers.[29] Images were reoriented to short-axis images and 17 myocardial segments were defined on images of tracer uptake between 5-10 minutes post injection. Obtained segment templates were projected onto all frames of the dynamic emission scan to extract segmental time-activity curves, which were fitted using a single tissue compartment model.[30] The rate constant k_2, representing the rate of transfer of radioactivity from tissue to blood, was used to derive myocardial oxygen consumption (MVO_2) as described previously.[29]

Myocardial efficiency

The combination of PET-derived MVO_2 and CMR-derived mechanical EW enables calculation of myocardial external efficiency,

$$\mathrm{MEE} = \frac{\mathrm{EW} \cdot \mathrm{HR} \cdot 1.33 \cdot 10^{-4}}{\mathrm{MVO}_2 \cdot \mathrm{LVM} \cdot 20}$$

in which *HR* is the heart rate and the constants represent the caloric equivalent of 1 mmHg·mL EW, which is $1.33 \cdot 10^{-4}$ J, whereas 1 mL O_2 corresponds to 20 J.[31]

Accuracy and reproducibility of PET/CMR analyses

The combination of PET/CMR analyses allow non-invasive determination of myocardial efficiency, which is the ratio of cardiac work and MVO_2.[31] Accurate measurement of LV volumes is important for the assessment of cardiac work. Cardiac CMR is considered the gold standard technique for LV volume measurements, because of the excellent accuracy and reproducibility of this technique.[32, 33]

In order to test the reproducibility of both imaging modalities in our study, three patients per group were randomly selected and PET/CMR images were analyzed by two operators independently from each other. The intra- and inter-observer agreements of different PET/CMR parameters were high (Table *2*).

Two different PET scanners were used to obtain values for k_2 for the $MYBPC3_{mut}$ carriers previously[23], and for the $MYH7_{mut}$ carriers. When comparing data from different scanners linearity issues and partial volume effects should be kept in mind. We have carefully checked these two parameters in previous studies. Regarding linearity issues, care was taken to ensure that the injected dose was within the linear range of the scanners used for both groups. For the controls and $MYBPC3_{mut}$ carriers, activity was half of that typically used for ^{15}O-water scans in these patients, ruling out linearity issues. For the $MYH7_{mut}$ group, dose was confirmed to be within the linear range of the scanner as confirmed in an earlier study using this scanner.[34] With respect to partial volume effects, the regions of interest (ROIs) in the aorta were 10 mm in diameter, whilst the aorta itself is typically ~25 mm in diameter. By placing the ROIs in the center of the aorta, partial volume effects are expected to be negligible as the ROIs were placed at least 8 mm from the edge of the aorta. Myocardial ROIs can suffer from partial volume effects, but these effects will only affect the absolute scaling of the time-activity curves, not the shape. Since we are evaluating k_2 i.e. washout of activity from tissue, absolute scaling plays no role in our estimation of k_2, as k_2 is estimated from the shape of the curve, not the height. This has been confirmed in an earlier study for ^{15}O-water, a tracer for which washout rate is the parameter of interest, as well.[35]

In order to keep the same scanning conditions, a standardized protocol was used for both imaging techniques. To reduce confounding effects on MVO_2, all PET-acquisitions were performed after overnight fasting of patients. Finally, we have proven experience with measurements of myocardial efficiency in HCM and carriers.[23, 36, 37]

Table 2. Intra-observer and inter-observer reliability for CMR and PET parameters

	Intra-observer variability		Inter-observer variability	
	ICC (95%-CI)	***P-value***	***ICC (95%-CI)***	***P-value***
CMR parameters				
LVEDV (mL·m^{-2})	0.96 (0.82-0.99)	<0.001	0.77 (-0.05-0.95)	<0.001
LVESV (mL·m^{-2})	0.97 (0.88-0.99)	<0.001	0.76 (-0.05-0.95)	<0.001
SV (mL·m^{-2})	0.94 (0.75-0.99)	<0.001	0.70 (0.18-0.92)	<0.01
LVM (g·m^{-2})	0.93 (0.53-0.99)	<0.001	0.81 (0.38-0.95)	<0.01
LVEF (%)	0.97 (0.87-0.99)	<0.001	0.78 (0.34-0.95)	<0.01
PET parameter				
Global k2	0.97 (0.39-0.99)	<0.001	0.99 (0.98-1.00)	<0.001

ICC, interclass correlation; CI, confidence interval; LV, left ventricular; LVEDV, LV end-diastolic volume; LVESV, LV end-systolic volume; SV, stroke volume; LVM, LV mass; LVEF, LV ejection fraction. Displayed values are interclass correlation coefficients.

Statistics

Data analysis and statistics were performed using the Prism version 5.0 (Graphpad Software, Inc., La Jolla, CA, USA) and SPSS version 20.0 (IMB, Armonk, NY, USA). The data regarding *in vitro* studies on myocardial tissue samples from manifest HCM patients are expressed as mean ± SD. *N* is the number of patients and *n* is the number of measured muscle strips. The datasets (*MYBPC3*$_{mut}$, *MYH7*$_{mut}$ and HCM$_{smn}$) were tested for normality using the Shapiro-Wilk test. Normality was assumed when $P > 0.05$ and variances were equal. The datasets regarding tension and ATPase activity were not violating this normality assumption, whereas TC datasets at both maximal and submaximal [Ca^{2+}] did. For this purpose, TC datasets had to be logarithmically transformed, which led to datasets following the normal distribution. As repeated sample assessments needed to be taken into account (multiple muscle strips were measured from one patient), multilevel analysis was performed using a linear mixed model procedure (SPSS) to investigate differences among groups.[38, 39] All analyses were performed on the individual measured muscle strips per data set. Data regarding phenotype-negative HCM mutation carriers were expressed by mean±SD. Statistics was performed on the individual patients. The datasets (*MYBPC3*$_{mut}$, *MYH7*$_{mut}$ and controls) were tested for normality as well using the Shapiro-Wilk test. The normality assumption was not violated ($P > 0.05$). A one-way ANOVA with Bonferroni post-hoc test was performed to investigate differences among groups. A *P*-value < 0.05 was considered significant.

Results

Characteristics of manifest HCM patients

Patient characteristics are presented in Table *1*. Hypertrophic obstructive cardiomyopathy was evident from septal thickness of ≥15 mm[40] and high LV outflow tract pressure gradient (normal value <30 mmHg).[41] There were no significant differences regarding the demographic and clinical parameters among the three manifest patient groups. The mutations present in the *MYBPC3*$_{mut}$ group are all so-called truncating mutations. Previous studies showed that truncating mutations result in a reduced expression of full-length cMyBP-C (i.e. haploinsufficiency).[42,43] The mutations present in the *MYH7*$_{mut}$ group are all missense mutations leading to poison peptides.[44]

Tension, ATPase activity and tension cost

Force production and ATPase activity were simultaneously measured in the tissue of 11 *MYBPC3*$_{mut}$, 9 *MYH7*$_{mut}$ and 6 HCM$_{smn}$ patients. The normality assumption was not violated ($P > 0.05$). Multilevel analysis revealed a significantly lower maximal tension (force production normalized to CSA) in *MYBPC3*$_{mut}$ ($^{*}P = 0.030$) and *MYH7*$_{mut}$ ($^{*}P < 0.0001$) compared with HCM$_{smn}$. In addition, maximal tension was significantly lower in *MYH7*$_{mut}$ than in *MYBPC3*$_{mut}$ ($^{\#}P < 0.0001$) (Figure *2A*). Figure *2B* shows that maximal ATPase activity did not differ between *MYBPC3*$_{mut}$ and HCM$_{smn}$, but it was significantly lower in *MYH7*$_{mut}$ compared with both *MYBPC3*$_{mut}$ ($^{\#}P < 0.0001$) and HCM$_{smn}$ ($^{*}P = 0.003$).

The ratio between maximal ATPase activity and tension represents the energetic cost of tension generation (Figure *2C*). The normality assumption was violated ($P < 0.05$), hence this dataset needed to be logarithmically transformed before multilevel analysis could be performed. Tension cost in *MYH7*$_{mut}$ was significantly higher than in HCM$_{smn}$ ($^{*}P < 0.0001$). Moreover, tension cost was significantly higher in *MYH7*$_{mut}$ than in *MYBPC3*$_{mut}$ ($^{\#}P = 0.01$).

Measurements of tension and ATPase activity were also performed at sub-maximal [Ca^{2+}] to assess tension cost in the physiological range of [Ca^{2+}]. The relation between tension and ATPase activity over the entire range of [Ca^{2+}] can be fitted to a linear equation.[45] The slope of the ATPase activity-tension curve represents tension cost over the entire [Ca^{2+}] range as can be appreciated from Figure *2D*. The vertical intercept represents ATPase activity at baseline. Baseline ATPase activity did not significantly differ among *MYBPC3*$_{mut}$, *MYH7*$_{mut}$ and HCM$_{smn}$ (6.8 ± 1.0, 4.5 ± 0.8, 7.5 ± 2.5 $\mu mol \cdot L^{-1} \cdot s^{-1}$, respectively). The individual slopes of all muscle strips were averaged per group and are shown in Figure *2E*. This dataset violated the normality assumption ($P < 0.05$), therefore requiring logarithmical transformation. Compared

with HCM_{smn}, the slope was significantly higher in $MYH7_{mut}$ (*P = 0.009). In addition, the slope of $MYH7_{mut}$ was also higher compared with $MYBPC3_{mut}$ ($^{\#}P$ = 0.036). Overall, data indicate that ATPase activity for force development is higher in mutation-positive than in mutation-negative preparations. The magnitude of the decrease in economy of sarcomere contraction depends on the affected gene at both saturating and sub-saturating calcium concentrations.

Characteristics of pre-hypertrophic mutation carriers and controls

A total of 28 asymptomatic pre-hypertrophic mutation carriers and 14 genotype-negative relatives were included in the study. The pre-hypertrophic *MYBPC3* mutation carriers all harbor the truncating mutation c.2373dupG, which was also present in samples from two manifest HCM patients (Table *1*). Although the mutations present in pre-hypertrophic mutation carriers (Table *3*) and in manifest HCM patients (Table *1*) were not exactly the same, the type of mutation was similar in both groups as all *MYBPC3* mutations were *truncating* mutations and *MYH7* mutations were *missense* mutations. Average characteristics of the groups are shown in Table *3*. The LVM index was comparable between $MYBPC3_{mut}$, $MYH7_{mut}$, and controls, as was stroke volume index and LV ejection fraction. No differences were observed with respect to end-diastolic wall thickness (both septal and lateral walls, Table *3*) between groups. Moreover, myocardium of all subjects displayed no late gadolinium enhancement.

Haemodynamics and metabolic characteristics, obtained during [^{11}C]-acetate PET acquisition, of the groups are depicted in Table *4*. Blood pressure, heart rate, and rate-pressure product were significantly lower in $MYH7_{mut}$ than in controls. Mean arterial pressure was significantly lower in $MYH7_{mut}$ than in $MYBPC3_{mut}$. Fasting glucose, free fatty acids, lactate, haemoglobin and NT-proBNP were comparable between groups. Figure *3* shows representative CMR and [^{11}C]-acetate PET images of the three separate groups. No structural differences were present between groups, as can be seen on the modified four-chamber views. k_2, representing the rate of [^{11}C]-acetate washout, tended to be higher in both mutation carrier groups, indicating a higher oxygen consumption. It did not significantly differ from controls.

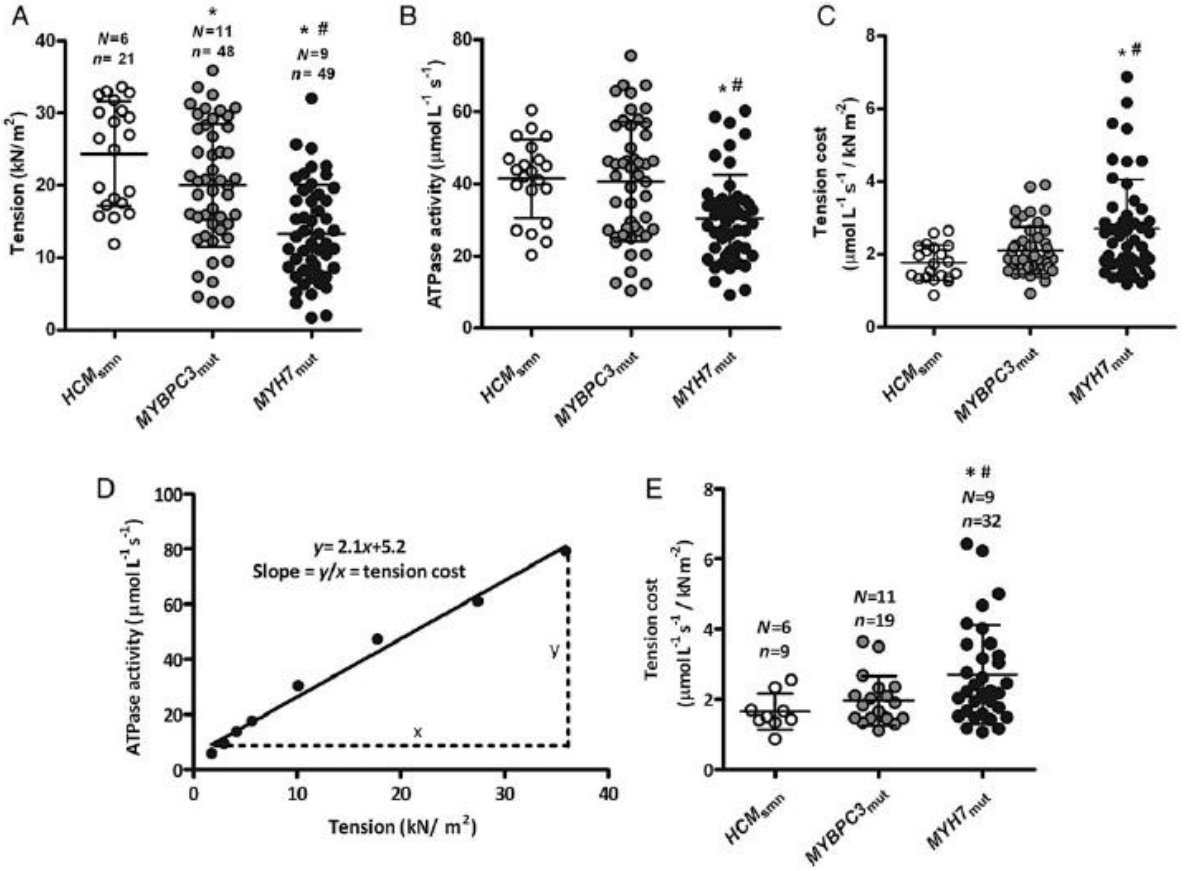

Figure 2. Sarcomere contractile and energetic properties in manifest HCM. *N*, number of patients; *n*, number of multicellular muscle strips. Data are presented as mean + SD, *vs. HCM_{smn} and # vs. $MYBPC3_{mut}$. (A) Maximal tension. (B) Maximal ATPase activity. (C) Maximal TC. (D) An example of the relation between tension and ATPase activity over the entire range of $[Ca^{2+}]$. (E) The average slopes of the ATPase activity–tension relations in MYBPC3mut, MYH7mut, and HCMsmn.

Table 3. Characteristics of pre-hypertrophic mutation carriers and controls

	***MYBPC3*$_{mut}$ (*n* = 14)**	***MYH7*$_{mut}$ (*n* = 14)**	**Controls (*n* = 14)**
Mutation	c.2373dupG	c.4130C>T (n=6) c.5135G>A (n=3) c.1207C>T (n=3) c.1727A>G (n=1) c.4130C>T (n=1)	
Sex (M)	4 (29%)*	3 (21%)*	9 (64%)
Age	37 ± 13	36 ± 13*	48 ± 11
LVEDV index (mL·m^{-2})	89 ± 13	83 ± 8	93 ± 15
LVESV index (mL·m^{-2})	36 ± 8	33 ± 3	36 ± 10
SV index (mL·m^{-2})	53 ± 7	51 ± 7	57 ± 7
LVEF (%)	60 ± 4	61 ± 3	62 ± 5
LVM index (g·m^{-2})	47 ± 7	50 ± 7	49 ± 6
EDWT septal (mm)	6.1 ± 0.8	6.6 ± 0.9	6.2 ± 0.8
EDWT lateral (mm)	5.3 ± 0.6	5.9 ± 0.7	5.7 ± 0.6
LGE (%)	0	0	0

Data are presented as mean ± SD or *n* (%). M, men; LVEDV, LV end-diastolic volume; LVESV, LV end-systolic volume; SV, stroke volume; LVEF, LV ejection fraction; LVM, LV mass; EDWT, end-diastolic wall thickness; LGE, late gadolinium enhancement. **P* < 0.05 vs. controls.

Table 4. Haemodynamic and metabolic characteristics of carriers and controls

	***MYBPC3*$_{mut}$ (*n* = 14)**	***MYH7*$_{mut}$ (*n* = 14)**	**Controls (*n* = 14)**
Systolic BP (mmHg)	118 ± 14	104 ± 10*$^{\#}$	123 ± 13
Diastolic BP (mmHg)	68 ± 8	61 ± 5*	71 ± 8
MAP (mmHg)	84 ± 9	76 ± 6*$^{\#}$	88 ± 8
Heart rate (bpm)	62 ± 8	60 ± 9*	69 ± 10
RPP	7317 ± 1174	6258 ± 1403*	8453 ± 1590
k_2 (per minute)	0.09 ± 0.02	0.09 ± 0.02	0.08 ± 0.02
NT-proBNP (ng·L^{-1})	71 ± 57	72 ± 45	63 ± 55
Hb (mmol·L^{-1})	8.3 ± 0.8	8.8 ± 0.9	8.3 ± 0.4
Glucose (mmol·L^{-1})	5.0 ± 0.7	5.1 ± 0.5	5.5 ± 0.8
FFA (mmol·L^{-1})	0.67 ± 0.26	0.51 ± 0.21	0.55 ± 0.26
Lactate (mmol·L^{-1})	1.1 ± 0.3	1.3 ± 0.5	1.4 ± 0.6

Data are presented as mean ± SD. BP, blood pressure; MAP, mean arterial pressure; RPP, rate-pressure product; k_2, average [^{11}C]-acetate clearance rate constant; NT-proBNP, NH_2-terminal pro-brain natriuretic peptide; Hb, haemoglobin; FFA, free fatty acid. **P* < 0.05 vs controls; $^{\#}$*P* < 0.05 between carrier groups.

External work, myocardial oxygen consumption and myocardial efficiency

Figure *4A* shows that external work was significantly lower in *MYBPC3*$_{mut}$ (*p = 0.008) and *MYH7*$_{mut}$ (**P* < 0.0001) carriers compared with controls. External work was lowest in *MYH7*$_{mut}$ carriers, but not significantly different from *MYBPC3*$_{mut}$ carriers (*P* = 0.34). Estimated MVO_2 did not significantly differ among groups (Figure *4B*). Myocardial efficiency was significantly lower in both *MYBPC3*$_{mut}$ (**P* < 0.0001) and *MYH7*$_{mut}$ (**P* < 0.0001) carriers compared with controls showing the lowest efficiency in *MYH7*$_{mut}$ carriers ($^{\#}P$ = 0.01 *MYH7*$_{mut}$ vs *MYBPC3*$_{mut}$; Figure *4C*).

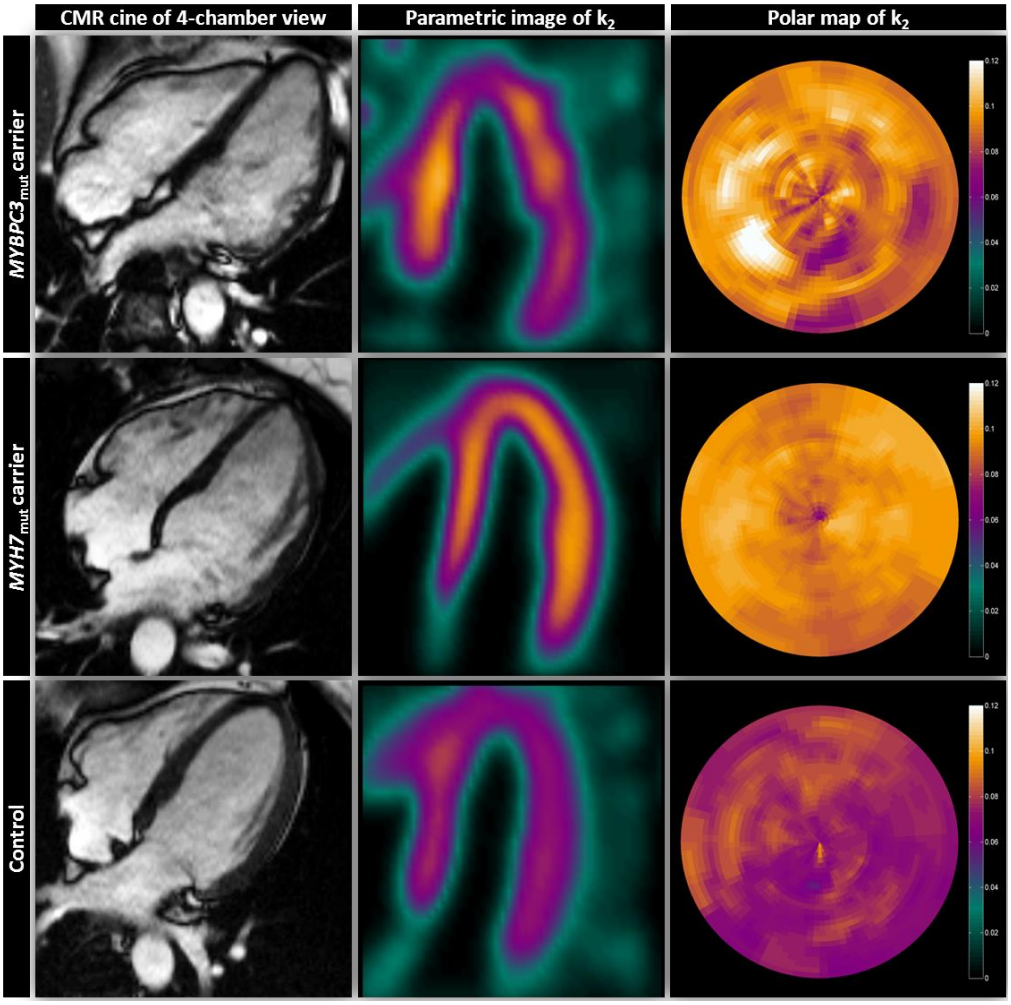

Figure 3. Cardiac imaging in a *MYBPC3*$_{mut}$ carrier, *MYH7*$_{mut}$ carrier, and a control. CMR-derived cardiac 4-chamber view and parametric images of [^{11}C]-acetate PET derived k_2 with corresponding polar maps.

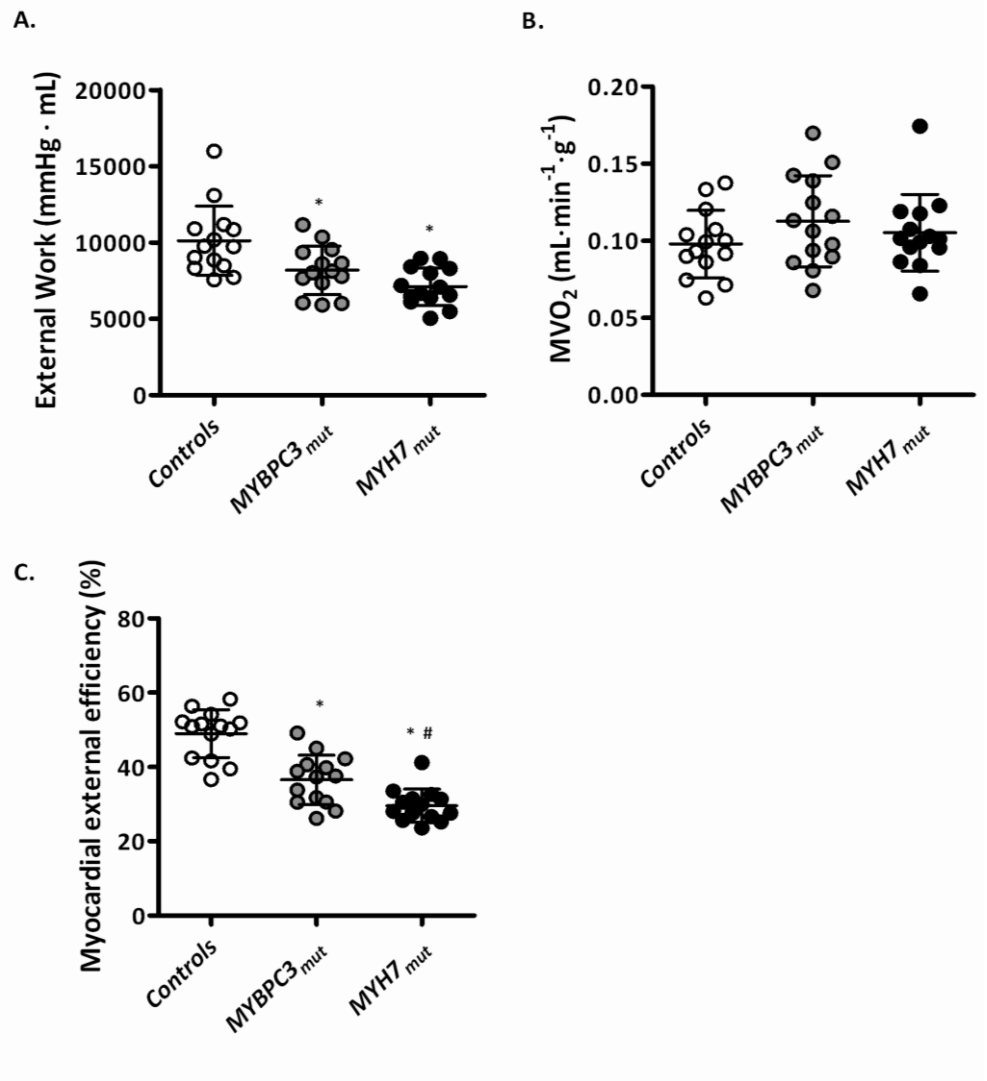

Figure 4. Cardiac work and energetics in pre-hypertrophic mutation carriers and controls. Data are presented as individual patients and with mean ± SD. **A.** External work. **B.** Estimated MVO_2. **C.** Myocardial efficiency. *vs. controls and #vs. *MYBPC3*$_{mut}$.

Discussion

We performed a comprehensive investigation of the impact of sarcomere mutations on energetic cost of cardiac contraction. By encompassing observations at the level of the myocardium to the level of the intact human, it was demonstrated that impaired energetic efficiency appears to be a fundamental consequence of sarcomere mutations. *In vitro* measurements of tension and ATPase activity in human cardiac muscle strips revealed a higher tension cost in sarcomere mutation-positive compared with sarcomere mutation-negative HCM. This suggests that energetic alterations are primarily related to the sarcomere mutation itself, rather than a non-specific feature of hypertrophied myocardium. Tension cost of sarcomere contraction was highest in myocardium harbouring mutations in *MYH7* compared with *MYBPC3*. Furthermore, non-invasive quantification of myocardial efficiency by use of [^{11}C]-acetate PET and CMR imaging in pre-hypertrophic mutation carriers revealed a significantly lower myocardial efficiency in both *MYH7*$_{mut}$ and *MYBPC3*$_{mut}$ compared with controls. The present results provide evidence that sarcomere mutations perturb the energetics of cardiac contractility in human myocardium. The reduction in myocardial efficiency was more prominent in the *MYH7*$_{mut}$ than in the *MYBPC3*$_{mut}$ group, at both the pre-hypertrophic and advanced stage of the disease, and may underlie differences observed in disease onset between these groups.

These findings imply that the increase in the energetic cost of sarcomere contraction depends on the affected gene. In addition, detection of reduced myocardial efficiency in pre-hypertrophic individuals carrying a sarcomere mutation suggests a potential target for treatment at an early stage of HCM disease.

Contractile function

Permeabilized cardiac multicellular muscle strips from manifest HCM patients with *MYBPC3* or *MYH7* mutations showed significantly lower maximal tension development compared with muscle strips from patients without sarcomere mutations. This is in line with the previously found decrease in maximal tension in single human cardiac cells harbouring *MYBPC3* and *MYH7* mutations, compared with non-failing donor cardiomyocytes.[39,42,46–48] The decrease in maximal tension was most prominent in *MYH7*$_{mut}$ muscle (Figure *2A*). In accordance with the *in vitro* measurements of force development in cardiac muscle strips, *in vivo* external work was significantly lower in both pre-hypertrophic mutation carrier groups compared with healthy controls, and the reduction in cardiac work was more prominent in *MYH7*$_{mut}$ than in *MYBPC3*$_{mut}$ (Figure *4A*). Overall, these data suggest that mutations in

thick filament proteins reduce the force-generating capacity of the myocardium even before the development of hypertrophy.

Cardiac energy utilization

ATPase activity in *MYBPC3*$_{mut}$ did not differ compared with HCM$_{smn}$ and was lowest in *MYH7*$_{mut}$. Although no increase was observed in ATPase activity in sarcomere mutation-positive myocardium compared with sarcomere mutation-negative samples, TC was significantly increased in both *MYH7*$_{mut}$ and *MYBPC3*$_{mut}$ compared with HCM$_{smn}$. The increase in TC, explained primarily by a reduction in maximal force-generating capacity, was largest in HCM caused by *MYH7* mutations.

The present data show for the first time that energetic cost of contraction is increased due to an imbalance between force-generating capacity and ATPase activity in sarcomere mutation-positive human HCM myocardium. Our findings are in line with previous results using similar measurements of ATPase activity and force development in muscle strips from transgenic mouse models harbouring mutations in *TNNT2*.[49,50] In these mouse models, the increase in TC in mice with a *TNNT2* mutation was explained by a significant decrease in force production and no change[49] or only a minor increase[50] in ATPase activity. The observation that changes in energetic cost of contraction are mostly due to a drop in force-generating capacity is supported by a previous *in vitro* motility and ATPase assay in human HCM tissue with a *MYH7* mutation. It was found that actin sliding velocity lagged behind ATPase activity.[51] In addition, an *in vitro* functional study[52] confirmed a higher rate of acto-myosin dissociation in skinned myofibrillar preparations harbouring a *MYH7* mutation, which relates to a drop in force production and increased energetic cost of contraction.[53,54]

Different parameters were determined within our *in vitro* analysis of local sarcomere energetics (ATPase activity and isometric tension) and *in vivo* analysis of global myocardial energetics (oxygen consumption and cardiac work production) to assess efficiency of cardiac performance. Nevertheless, in accordance with our *in vitro* analysis of TC*,* studies in pre-hypertrophic *MYH7*$_{mut}$ carriers showed a more severe reduction in myocardial efficiency compared with *MYBPC3*$_{mut}$ carriers (Figure *4C*). The decrease in myocardial efficiency was largely explained by a reduction in cardiac work rather than an increase in MVO_2. To date, only a few non-invasive *in vivo* studies of myocardial energetics in genotype-positive, phenotype-negative mutation carriers have been performed.[20,23] A study by Crilley and coworkers showed that PCr/ATP was reduced in phenotype-negative mutation carriers as well.[20] However, no distinction could be made between carriers with different gene-mutations due to the small numbers. Another study demonstrated that alterations in PCr/ATP in HCM are correlated with the presence of fibrotic areas in the

myocardium.[55] In the present study, however, patients underwent late gadolinium enhancement imaging to rule out the presence of replacement fibrosis.

Overall, our *in vitro* results using tissue of phenotype-positive HCM subjects, revealed an increase in TC based on a misbalance between force-generating capacity and ATPase activity. Therefore, it could be one of the mechanisms for global myocardial deficiency. Already in an early pre-hypertrophic phase of HCM, sarcomere mutations lead to a decrease in global myocardial efficiency as there is less work produced, while there is no change in energy utilization compared with healthy controls. Therefore, our *in vivo* findings suggest that disturbance of myocardial efficiency is indeed a primary event before onset of cardiac remodelling. Disturbances in myocardial energetics seem to be more prominent in HCM with *MYH7* compared with *MYBPC3* mutations and may explain the difference in disease onset between these two groups.

Study limitations

Myocardial ischaemia has been associated with alterations of myocardial metabolism and may also influence myocardial efficiency. In the present study, no measurements of myocardial perfusion were performed in both phenotype-negative carrier groups and healthy controls to rule out myocardial ischaemia. On the other hand, patients were considered to be at low risk for coronary artery disease based on clinical history and ECG findings. No regional wall motion abnormalities were seen on CMR. Furthermore, there was no fibrosis present as demonstrated by late gadolinium enhancement imaging (Table *3*).

The number of patients included in this study was relatively small, and therefore, results should be interpreted with care. Nonetheless, group sample sizes were large enough to provide evidence of mutation-specific abnormalities in myocardial energetic cost of contraction in human HCM. In the *in vivo* imaging study, groups were not matched for age and gender. Pre-hypertrophic mutation carriers were significantly younger and more women were included compared with the control group. However, based on the fact that myocardial energetics deteriorates with aging[56,57], the reduction in myocardial efficiency observed in mutation carriers would be even larger when compared with age-matched controls.

Clinical implications

The present results show that sarcomere energetics is affected mostly in HCM with *MYH7* mutations, in the manifest stage of the disease. Moreover, *MYH7* mutations seem to result in a more severe clinical phenotype than *MYBPC3* mutations, as septal thickness was slightly higher in $MYH7_{mut}$ compared with $MYBPC3_{mut}$ HCM patients (Table *1*). However, patients with the same *MYH7* mutation showed a

diverse disease onset as a 28-year old patient with the c.2080C>T mutation had the highest septal thickness (49 mm), while another patient with the same mutation was operated at 81 years of age. Strikingly, septal thickness in this older patient was only 19 mm (Table *1*).

Recently, a pharmacological intervention study[58] was performed in HCM patients using perhexiline, a modulator of substrate metabolism, shifting metabolism from free fatty acids to glucose.[59] Perhexiline treatment improved myocardial energetics and exercise capacity. The present results show that disturbance in myocardial efficiency is already present in pre-hypertrophic mutation carriers and may be a primary trigger for the development of the HCM phenotype. Both *in vivo* at the pre-hypertrophic stage and *in vitro* in manifest HCM, the present study provides evidence that the degree of impaired efficiency of contraction depends on the affected gene. These data warrant further clinical studies towards gene-specific metabolic treatment at an early phase of the disease process.

Source of funding

This work was supported by the 7th Framework Program of the European Union ("BIG-HEART," grant agreement 241577), Netherlands Organization for Scientific Research (NWO; VIDI grant) and Netherlands Heart Foundation ("Dekker Grant" grant agreement 2011T33).

Conflict of interest

None declared.

References

1. Maron BJ, Towbin JA, Thiene G, Antzelevitch C, Corrado D, Arnett D, Moss AJ, Seidman CE, Young JB. Contemporary definitions and classification of the cardiomyopathies: an American Heart Association Scientific Statement from the Council on Clinical Cardiology, Heart Failure and Transplantation Committee; Quality of Care and Outcomes Research and Functional Genomics and Translational Biology Interdisciplinary Working Groups; and Council on Epidemiology and Prevention. *Circulation* 2006;113:1807–1816.
2. Brigden W. Uncommon myocardial diseases: the non-coronary cardiomyopathies. *Lancet* 1957;273:1243–1249.
3. Geisterfer-Lowrance AA, Kass S, Tanigawa G, Vosberg HP, McKenna W, Seidman CE, Seidman JG. A molecular basis for familial hypertrophic cardiomyopathy: a beta cardiac myosin heavy chain gene missense mutation. *Cell* 1990;62:999–1006.
4. Alcalai R, Seidman JG, Seidman CE. Genetic basis of hypertrophic cardiomyopathy: from bench to the clinics. *J Cardiovasc Electrophysiol* 2008;19:104–110.
5. Charron P, Dubourg O, Desnos M, Bennaceur M, Carrier L, Camproux AC, Isnard R, Hagege A, Langlard JM, Bonne G, Richard P, Hainque B, Bouhour JB, Schwartz K, Komajda M. Clinical features and prognostic implications of familial hypertrophic cardiomyopathy related to the cardiac myosin-binding protein C gene. *Circulation* 1998;97:2230–2236.
6. Marian AJ, Salek L, Lutucuta S. Molecular genetics and pathogenesis of hypertrophic cardiomyopathy. *Minerva Med* 2001;92:435–451.
7. Michels M, Soliman OII, Phefferkorn J, Hoedemaekers YM, Kofflard MJ, Dooijes D, Majoor-Krakauer D, Ten Cate FJ. Disease penetrance and risk stratification for sudden cardiac death in asymptomatic hypertrophic cardiomyopathy mutation carriers. *Eur Heart J* 2009;30:2593–8.
8. Niimura H, Bachinski LL, Sangwatanaroj S, Watkins H, Chudley AE, McKenna W, Kristinsson A, Roberts R, Sole M, Maron BJ, Seidman JG, Seidman CE. Mutations in the gene for cardiac myosin-binding protein C and late-onset familial hypertrophic cardiomyopathy. *N Engl J Med* 1998;338:1248–1257.
9. Niimura H, Patton KK, McKenna WJ, Soults J, Maron BJ, Seidman JG, Seidman CE. Sarcomere protein gene mutations in hypertrophic cardiomyopathy of the elderly. *Circulation* 2002;105:446–451.
10. Olson RE, Schwartz WB. Myocardial metabolism in congestive heart failure. *Medicine (Baltimore)* 1951;30:21–41.
11. Katz AM. Is the failing heart energy depleted? *Cardiol Clin* 1998;16:633–644.
12. Neubauer S, Horn M, Cramer M, Harre K, Newell JB, Peters W, Pabst T, Ertl G, Hahn D, Ingwall JS, Kochsiek K. Myocardial phosphocreatine-to-ATP ratio is a predictor of mortality in patients with dilated cardiomyopathy. *Circulation* 1997;96:2190–2196.
13. Kalsi KK, Smolenski RT, Pritchard RD, Khaghani A, Seymour AM, Yacoub MH. Energetics and function of the failing human heart with dilated or hypertrophic cardiomyopathy. *Eur J Clin Invest* 1999;29:469–477.
14. Ashrafian H, Redwood C, Blair E, Watkins H. Hypertrophic cardiomyopathy:a paradigm for myocardial energy depletion. *Trends Genet* 2003;19:263–268.
15. Ingwall JS. Energy metabolism in heart failure and remodelling. *Cardiovasc Res* 2009;81:412–419.
16. Javadpour MM, Tardiff JC, Pinz I, Ingwall JS. Decreased energetics in murine hearts bearing the R92Q mutation in cardiac troponin T. *J Clin Invest* 2003;112:768–775.

17. He H, Javadpour MM, Latif F, Tardiff JC, Ingwall JS. R-92L and R-92W mutations in cardiac troponin T lead to distinct energetic phenotypes in intact mouse hearts. *Biophys J* 2007;93:1834–1844.
18. Spindler M, Saupe KW, Christe ME, Sweeney HL, Seidman CE, Seidman JG, Ingwall JS. Diastolic dysfunction and altered energetics in the alphaMHC403/+ mouse model of familial hypertrophic cardiomyopathy. *J Clin Invest* 1998;101:1775–1783.
19. Luedde M, Flögel U, Knorr M, Grundt C, Hippe H-J, Brors B, Frank D, Haselmann U, Antony C, Voelkers M, Schrader J, Most P, Lemmer B, Katus HA, Frey N. Decreased contractility due to energy deprivation in a transgenic rat model of hypertrophic cardiomyopathy. *J Mol Med* 2009;87:411–422.
20. Crilley JG, Boehm EA, Blair E, Rajagopalan B, Blamire AM, Styles P, McKenna WJ, Ostman-Smith I, Clarke K, Watkins H. Hypertrophic cardiomyopathy due to sarcomeric gene mutations is characterized by impaired energy metabolism irrespective of the degree of hypertrophy. *J Am Coll Cardiol* 2003;41:1776–1782.
21. Jung WI, Hoess T, Bunse M, Widmaier S, Sieverding L, Breuer J, Apitz J, Schmidt O, van Erckelens F, Dietze GJ, Lutz O. Differences in cardiac energetics between patients with familial and nonfamilial hypertrophic cardiomyopathy. *Circulation* 2000;101:E121.
22. Jung WI, Sieverding L, Breuer J, Hoess T, Widmaier S, Schmidt O, Bunse M, van Erckelens F, Apitz J, Lutz O, Dietze GJ. 31P NMR spectroscopy detects metabolic abnormalities in asymptomatic patients with hypertrophic cardiomyopathy. *Circulation* 1998;97:2536–2542.
23. Timmer SA, Germans T, Brouwer WP, Lubberink M, van der Velden J, Wilde AA, Christiaans I, Lammertsma AA, Knaapen P, van Rossum AC. Carriers of the hypertrophic cardiomyopathy MYBPC3 mutation are characterized by reduced myocardial efficiency in the absence of hypertrophy and microvascular dysfunction. *Eur J Heart Fail* 2011;13:1283–1289.
24. Potma EJ, Stienen GJ, Barends JP, Elzinga G. Myofibrillar ATPase activity and mechanical performance of skinned fibres from rabbit psoas muscle. *J Physiol* 1994;474:303–317.
25. Van der Velden J, Moorman AF, Stienen GJ. Age-dependent changes in myosin composition correlate with enhanced economy of contraction in guinea-pig hearts. *J Physiol* 1998;507:497–510.
26. Narolska NA, van Loon RB, Boontje NM, Zaremba R, Penas SE, Russell J, Spiegelenberg SR, Huybregts MA, Visser FC, de Jong JW, van der Velden J, Stienen GJM. Myocardial contraction is 5-fold more economical in ventricular than in atrial human tissue. *Cardiovasc Res* 2005;65:221–229.
27. Potma EJ, van Graas IA, Stienen GJ. Effects of pH on myofibrillar ATPase activity in fast and slow skeletal muscle fibers of the rabbit. *Biophys J* 1994;67:2404–2410.
28. Marcus JT, DeWaal LK, Gotte MJ, van der Geest RJ, Heethaar RM, van Rossum AC. MRI-derived left ventricular function parameters and mass in healthy young adults: relation with gender and body size. *Int J Card Imaging* 1999;15:411–419.
29. Sun KT, Yeatman LA, Buxton DB, Chen K, Johnson JA, Huang SC, Kofoed KF, Weismueller S, Czernin J, Phelps ME, Schelbert HR. Simultaneous measurement of myocardial oxygen consumption and blood flow using [1-carbon-11]acetate. *J Nucl Med* 1998;39:272–280.
30. Timmer SAJ, Lubberink M, van Rossum AC, Lammertsma AA, Knaapen P. Reappraisal of a single-tissue compartment model for estimation of myocardial oxygen consumption by [^{11}C]acetate PET: an alternative to conventional monoexponential curve fitting. *Nucl Med Commun* 2011;32:59–62.
31. Knaapen P, Germans T, Knuuti J, Paulus WJ, Dijkmans PA, Allaart CP, Lammertsma AA, Visser FC. Myocardial energetics and efficiency: current status of the noninvasive approach. *Circulation* 2007;115:918–927.

32. Maceira AM, Prasad SK, Khan M, Pennell DJ. Reference right ventricular systolic and diastolic function normalized to age, gender and body surface area from steady-state free precession cardiovascular magnetic resonance. *Eur Heart J* 2006;27:2879–2888.
33. Grothues F, Smith GC, Moon JC., Bellenger NG, Collins P, Klein HU, Pennell DJ. Comparison of interstudy reproducibility of cardiovascular magnetic resonance with two-dimensional echocardiography in normal subjects and in patients with heart failure or left ventricular hypertrophy. *Am J Cardiol* 2002;90:29–34.
34. Lubberink M, van der Veldt A, Knaapen P, Harms H, Smit E, Hendrikse H, Lammertsma A. Measurement of tumor and myocardial perfusion using 15O-water and a clinical PET-CT scanner. *Soc Nucl Med Annu Meet Abstr* 2009;50:238.
35. Lubberink M, Harms HJ, Halbmeijer R, de Haan S, Knaapen P, Lammertsma AA. Low-dose quantitative myocardial blood flow imaging using 15O-water and PET without attenuation correction. *J Nucl Med* 2010;51:575–80.
36. Timmer SAJ, Knaapen P, Germans T, Dijkmans PA, Lubberink M, Ten Berg JM, Ten Cate FJ, Rüssel IK, Götte MJW, Lammertsma AA, van Rossum AC. Effects of alcohol septal ablation on coronary microvascular function and myocardial energetics in hypertrophic obstructive cardiomyopathy. *Am J Physiol Heart Circ Physiol* 2011;301:129–137.
37. Timmer SAJ, Germans T, Götte MJW, Rüssel IK, Dijkmans PA, Lubberink M, ten Berg JM, ten Cate FJ, Lammertsma AA, Knaapen P, van Rossum AC. Determinants of myocardial energetics and efficiency in symptomatic hypertrophic cardiomyopathy. *Eur J Nucl Med Mol Imaging* 2010;37:779–788.
38. Sequeira V, Wijnker PJ, Nijenkamp LL, Kuster DW, Najafi A, Witjas-Paalberends R, Regan JA, Boontje N, Ten CF, Germans T, Carrier L, Sadayappan S, Van SM, Zaremba R, Foster DB, Murphy A, Poggesi C, dos Remedios CG, Stienen GJ, Ho CY, Michels M, Van der Velden J. Perturbed Length-Dependent Activation in Human Hypertrophic Cardiomyopathy with Missense Sarcomeric Gene Mutations. *Circ Res* 2013;112:1491–1505.
39. Witjas-Paalberends ER, Piroddi N, Stam K, van Dijk SJ, Oliviera VS, Ferrara C, Scellini B, Hazebroek M, Ten Cate FJ, Van SM, Dos RC, Niessen HW, Tesi C, Stienen GJM, Heymans S, Michels M, Poggesi C, Van der Velden J. Mutations in MYH7 reduce the force generating capacity of sarcomeres in human familial hypertrophic cardiomyopathy. *Cardiovasc Res* 2013;99:432–441.
40. Shub C, Klein AL, Zachariah PK, Bailey KR, Tajik AJ. Determination of left ventricular mass by echocardiography in a normal population: effect of age and sex in addition to body size. *Mayo Clin Proc* 1994;69:205–211.
41. Maron MS, Olivotto I, Zenovich AG, Link MS, Pandian NG, Kuvin JT, Nistri S, Cecchi F, Udelson JE, Maron BJ. Hypertrophic cardiomyopathy is predominantly a disease of left ventricular outflow tract obstruction. *Circulation* 2006;114:2232–2239.
42. Van Dijk SJ, Dooijes D, Dos RC, Michels M, Lamers JM, Winegrad S, Schlossarek S, Carrier L, Ten Cate FJ, Stienen GJM, Van der Velden J. Cardiac myosin-binding protein C mutations and hypertrophic cardiomyopathy: haploinsufficiency, deranged phosphorylation, and cardiomyocyte dysfunction. *Circulation* 2009;119:1473–1483.
43. Marston S, Copeland O, Jacques A, Livesey K, Tsang V, McKenna WJ, Jalilzadeh S, Carballo S, Redwood C, Watkins H. Evidence from human myectomy samples that MYBPC3 mutations cause hypertrophic cardiomyopathy through haploinsufficiency. *Circ Res* 2009;105:219–222.
44. Becker KD, Gottshall KR, Hickey R, Perriard JC, Chien KR. Point mutations in human beta cardiac myosin heavy chain have differential effects on sarcomeric structure and assembly: an ATP binding site change disrupts both thick and thin filaments, whereas hypertrophic cardiomyopathy mutations display normal assemb. *J Cell Biol* 1997;137:131–140.

45. De Tombe PP, Stienen GJM. Protein kinase A does not alter economy of force maintenance in skinned rat cardiac trabeculae. *Circ Res* 1995;76:734–741.
46. Hoskins AC, Jacques A, Bardswell SC, McKenna WJ, Tsang V, dos Remedios CG, Ehler E, Adams K, Jalilzadeh S, Avkiran M, Watkins H, Redwood C, Marston SB, Kentish JC. Normal passive viscoelasticity but abnormal myofibrillar force generation in human hypertrophic cardiomyopathy. *J Mol Cell Cardiol* 2010;49:737–745.
47. Kraft T, Witjas-Paalberends ER, Boontje NM, Tripathi S, Brandis A, Montag J, Hodgkinson JL, Francino A, Navarro-Lopez F, Brenner B, Stienen GJM, Van der Velden J. Familial hypertrophic cardiomyopathy: functional effects of myosin mutation R723G in cardiomyocytes. *J Mol Cell Cardiol* 2013;57:13–22.
48. Van Dijk SJ, Paalberends ER, Najafi A, Michels M, Sadayappan S, Carrier L, Boontje NM, Kuster DW, Van SM, Dooijes D, Dos RC, Ten Cate FJ, Stienen GJM, Van der Velden J. Mutation. *Circ Heart Fail* 2012;5:36–46.
49. Montgomery DE, Tardiff JC, Chandra M. Cardiac troponin T mutations: correlation between the type of mutation and the nature of myofilament dysfunction in transgenic mice. *J Physiol* 2001;536:583–592.
50. Chandra M, Tschirgi ML, Tardiff JC. Increase in tension-dependent ATP consumption induced by cardiac troponin T mutation. *Am J Physiol Heart Circ Physiol* 2005;289:112–119.
51. Keller DI, Coirault C, Rau T, Cheav T, Weyand M, Amann K, Lecarpentier Y, Richard P, Eschenhagen T, Carrier L. Human homozygous R403W mutant cardiac myosin presents disproportionate enhancement of mechanical and enzymatic properties. *J Mol Cell Cardiol* 2004;36:355–362.
52. Belus A, Piroddi N, Scellini B, Tesi C, Amati GD, Girolami F, Yacoub M, Cecchi F, Olivotto I, Poggesi C. The familial hypertrophic cardiomyopathy-associated myosin mutation R403Q accelerates tension generation and relaxation of human cardiac myofibrils. *J Physiol* 2008;586:3639–3644.
53. Brenner B. Effect of Ca2+ on cross-bridge turnover kinetics in skinned single rabbit psoas fibers: implications for regulation of muscle contraction. *Proc Natl Acad Sci* 1988;85:3265–3269.
54. Poggesi C, Tesi C, Stehle R. Sarcomeric determinants of striated muscle relaxation kinetics. *Pflugers Arch* 2005;449:505–517.
55. Esposito A, De Cobelli F, Perseghin G, Pieroni M, Belloni E, Mellone R, Canu T, Gentinetta F, Scifo P, Chimenti C, Frustaci A, Luzi L, Maseri A, Maschio A Del. Impaired left ventricular energy metabolism in patients with hypertrophic cardiomyopathy is related to the extension of fibrosis at delayed gadolinium-enhanced magnetic resonance imaging. *Heart* 2009;95:228–233.
56. Hollingsworth KG, Blamire AM, Keavney BD, Macgowan GA. Left ventricular torsion, energetics, and diastolic function in normal human aging. *Am J Physiol Heart Circ Physiol* 2012;302:885–892.
57. Schocke MF., Metzler B, Wolf C, Steinboeck P, Kremser C, Pachinger O, Jaschke W, Lukas P. Impact of aging on cardiac high-energy phosphate metabolism determined by phosphorus-31 2-dimensional chemical shift imaging (31P 2D CSI). *Magn Reson Imaging* 2003;21:553–559.
58. Abozguia K, Elliott P, McKenna W, Phan TT, Nallur-Shivu G, Ahmed I, Maher AR, Kaur K, Taylor J, Henning A, Ashrafian H, Watkins H, Frenneaux M. Metabolic modulator perhexiline corrects energy deficiency and improves exercise capacity in symptomatic hypertrophic cardiomyopathy. *Circulation* 2010;122:1562–1569.
59. Ashrafian H, Horowitz JD, Frenneaux MP. Perhexiline. *Cardiovasc Rev* 2007;25:76–97.